



Article

Fire Behavior and Adhesion of Magnesium Phosphate Coatings for the Protection of Steel Structures

Nicoleta Florentina Cirstea ¹, Alina Badanoiu ^{1,*}, Georgeta Voicu ¹, Robert Catalin Ciocoiu ² 
and Aurelian Cristian Boscornea ³ 

¹ Department Science and Engineering of Oxide Materials, Faculty of Chemical Engineering and Biotechnologies, University Politehnica of Bucharest, 060042 Bucharest, Romania

² Metallic Materials Science, Physical Metallurgy Department, Faculty of Science and Engineering of Materials, University Politehnica of Bucharest, 060042 Bucharest, Romania

³ Department Bioresources and Polymer Science, Faculty of Chemical Engineering and Biotechnologies, University Politehnica of Bucharest, 060042 Bucharest, Romania

* Correspondence: alina.badanoiu@upb.ro

Abstract: This paper presents the main properties of magnesium phosphate cements (MPCs) to be used as coatings for passive fire protection of steel structures. The influence of various additions, i.e., waste glass powder, fly ash, a styrene–acrylic dispersion, and expandable graphite, on the fire behavior and the adhesion to steel substrates of magnesium phosphate coatings is presented in this paper. The setting time of studied cements is extended when magnesia, the main component of MPCs, is partially replaced with fly ash or/and waste glass powder. The mineralogical composition of these cements, before and after thermal treatment at 1050 °C, was assessed by X-ray diffraction and could explain the changes in compressive strength, volume, and mass recorded for the thermally treated specimens. The studied magnesium phosphate coatings have a good adherence to the steel substrate (assessed by a pull-off test) both before and after direct contact with a flame (fire test) and decrease the temperature of the steel substrate by 30% with respect to the one recorded for the uncoated steel plate.

Keywords: fire protection; magnesium phosphate cement; steel; additions; adhesion strength



Citation: Cirstea, N.F.; Badanoiu, A.; Voicu, G.; Ciocoiu, R.C.; Boscornea, A.C. Fire Behavior and Adhesion of Magnesium Phosphate Coatings for the Protection of Steel Structures.

Appl. Sci. **2022**, *12*, 12620.

<https://doi.org/10.3390/app122412620>

Academic Editors: Luis Laim,
Aldina Santiago and Nicola Tondini

Received: 28 October 2022

Accepted: 6 December 2022

Published: 9 December 2022

Publisher's Note: MDPI stays neutral with regard to jurisdictional claims in published maps and institutional affiliations.



Copyright: © 2022 by the authors. Licensee MDPI, Basel, Switzerland. This article is an open access article distributed under the terms and conditions of the Creative Commons Attribution (CC BY) license (<https://creativecommons.org/licenses/by/4.0/>).

1. Introduction

Fire is essential for human life, but if not properly managed can lead to human life losses and the destruction of important materials. Fire protection in construction is of utmost importance, especially for those with steel structures, given the fact that steel starts to lose its mechanical properties when heated; thus, when the steel temperature exceeds 550–600 °C, it retains only about 50% of its ambient temperature strength [1–3]. Various passive fire protection materials can be applied to steel structures in order to improve their fire behavior; among them are cementitious coating mortars, plaster or silicate calcium boards, and intumescent coatings (organic or inorganic) [3–6]. According to Laim et al. [4], these materials should be cheap, non-hazardous, both during application and in the event of a fire (i.e., they should not emit toxic gases), and should remain undamaged and attached to the steel element as long as possible in order to ensure good insulation and protection.

Intumescent organic coatings (based on polymers) can easily be applied to various substrates and present an important swelling when exposed to heat [3]. Although this type of intumescent coating is frequently used today, it has some disadvantages, such as temperature limitation, the release of smoke and toxic fumes during heating, and, in some cases, the potential displacement of the protective char layer formed during the fire [3].

Inorganic intumescent coatings based on alkali silicates can also be used as passive fire protection; the main advantages of these types of materials relate to their good resistance to microorganisms and UV radiation [7], and opposite to the organic intumescent coatings,

they can perform at higher temperatures and release non-toxic water vapors during the intumescence process [3,6].

Intumescent alkali silicate pastes and mortars can also be used to limit the temperature increase in steel structures [5,8,9]; these materials, called alkali-activated borosilicate inorganic polymers (AABSIPs), can be obtained by the alkali activation of waste glass powder with a mixture of sodium hydroxide solution and borax. When AABSIPs are heated to temperatures between 400 and 600 °C or are put in direct contact with the flame, they exhibit an important swelling, i.e., the volume increases between 250% and 430% [5,10]; these coatings can effectively limit the increase in the carbon steel substrate temperature above that which is considered critical (550–600 °C) [5].

The main drawback of intumescent materials (organic or inorganic), which could limit their extensive use, is their higher price as compared with cementitious mortars, especially those based on portland cement. In order to enhance the thermal performance (reduce the thermal conductivity) of portland cement concrete/mortar, it is recommended to replace the normal aggregates with lightweight ones such as expanded polystyrene particles, vermiculite, perlite, etc. [4,11,12]. Nevertheless, the compressive strength and adhesion to metallic substrates of portland cement mortars with lightweight aggregates are small and decrease with the increase in temperature (although this decrease is smaller as compared with the one assessed for the control mortar—with normal aggregates). For example, for a cement mortar with 10–40% vermiculite, the compressive strength decrease was between 1.7% and 21.41% when the materials were heated to 300 °C and between 57.06% and 81.03% when the thermal treatment temperature was 900 °C [12].

In this respect, magnesium phosphate cement (MPC) is considered an interesting candidate for the fire protection of metallic structures [13–17]. MPCs have a higher adhesion to various types of substrates (including steel) compared to portland cement [16,17]. Moreover, this type of cement has a rapid setting, high early strength, long-term durability, and good abrasion resistance [17–20]. Thus, magnesium phosphate cements are used in various applications, such as the rapid repair of airport runways, bridges, and tunnels [18,21,22] but also as bone or dental cement due to their good biocompatibility [23–25].

MPC hardens due to an acid–base reaction between magnesium oxide and phosphoric acid or phosphate salts in the presence of water [18]. Ammonium dihydrogen phosphate ($\text{NH}_4\text{H}_2\text{PO}_4$) and potassium dihydrogen phosphate (KH_2PO_4) are the most frequently used phosphate salts for MPC manufacture. Dai et al. [14] prepared an $\text{NH}_4\text{H}_2\text{PO}_4$ -based MPC and tested it as a fire-retardant coating for steel structures. The fireproof performance of this coating was adequate, and the use of expanded vermiculite as a lightweight aggregate improved the fire performance of this material.

The main drawback when using $\text{NH}_4\text{H}_2\text{PO}_4$ as a precursor for MPC manufacture is the release of ammonia (toxic gas) both during its preparation and after hardening. Therefore, in a previous study, we used KH_2PO_4 to prepare magnesium phosphate cement (MPC) using dead burnt magnesia as a precursor and calcium magnesium phosphate cements (CMPC) based on calcined dolomite [16]. The obtained results showed that the coatings based on MPC and CMPC (without borax addition) applied to a steel plate, tested in direct contact with a flame, prevented the temperature of the metal substrate from increasing over 500 °C. Moreover, during the entire period of the test (45 min), no exfoliation was noticed, i.e., the coatings had good adhesion to the metal substrate. Additionally, although the MPC coating did not crack or delaminate in the area where it was in direct contact with the flame, visible cracks were formed on the adjacent zones during the fire test.

In this respect, in this study, we aimed to improve several properties of MPCs based on dead burnt magnesia and KH_2PO_4 , i.e., to increase the setting time of the cement paste as well as its adherence to the steel substrate before, during, and after fire test.

Starting from previously obtained results [16] and based on the available information in the literature, in the formulation of MPC coatings studied in this research, other components were added: a styrene–acrylic dispersion (Ac) with the aim of improving the elastic behavior of the MPC coating and at the same time to increase the MPC setting

time [26]; fly ash in order to extend the setting time and to improve the MPC adhesion to the substrate [17,27]; waste glass powder in order to extend the setting time, to improve the mechanical properties and to slightly decrease the melting temperature of the material [15,28]; and expandable graphite in order to increase the porosity of coating during the fire test [29]. To the best of our knowledge this is a new approach in the attempt to improve the above-mentioned properties.

Thus, in this paper we present information regarding the ability of these coatings to prevent the increase in the substrate (carbon steel plate) temperature, along with the influence exerted by high temperatures on the compressive strength of MPCs, and volume and mass changes in correlation with the change of mineralogical composition (assessed by XRD) as well as on the adhesive strength of the coatings to steel substrate.

2. Materials and Methods

The materials used in this research were:

- Magnesia (M) obtained by the thermal treatment of magnesite at 1500 °C. The magnesia was purchased from Tremag, Tulcea, Romania. The main crystalline component assessed by XRD was MgO (Figure 1).
- Fly ash (F), waste resulting from coal combustion in a power plant; the mineralogical composition of this material comprises SiO₂, Al₂SiO₅, and CaSO₄ (Figure 1).
- Waste glass powder (S)—obtained by the grinding of soda–lime glass culets, up to a fineness corresponding to a Blaine specific surface area of 2858 cm²/g.
- KH₂PO₄ (MKP)—chemical reagent ACS grade (Sigma-Aldrich, ≥99%—Darmstadt, Germany).
- Borax (Na₂B₄O₇·10H₂O) (B)—chemical reagent ACS grade from Sigma-Aldrich, conc. > 99.5%.
- Styrene–acrylic dispersion Acronal S562 (Ac), from BASF (Ludwigshafen, Germany), solid content 49–51%, particle size range: <0.1–10 µm; density 1.04 kg/m³, and viscosity 800 mPa·s (23 °C, 100 1/s).
- Expandable graphite (EG) was prepared according to the method proposed by Hung et al. [30]. This method consists of the treatment of graphite with nitric acid and sulfuric acid under continuous stirring for 6 h. Expandable graphite is obtained by filtration, washing the sediment with water, and drying at 70 °C for 24 h. The graphite was obtained from ACROS ORGANICS (Geel, Belgium).

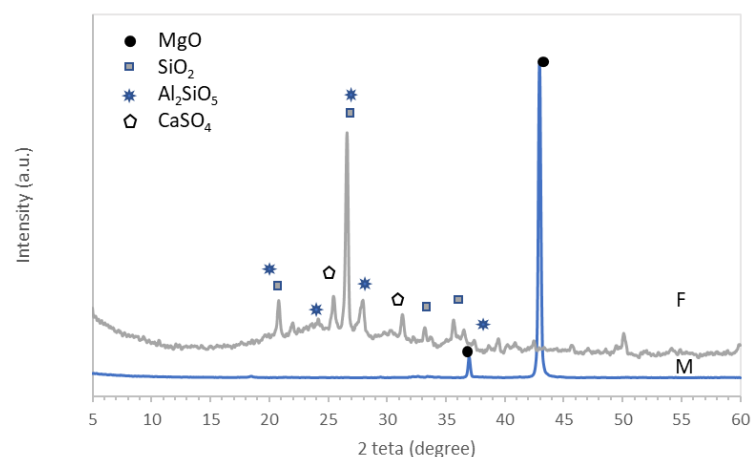


Figure 1. XRD patterns of magnesia (M) and fly ash (F).

The compositions of the studied MPCs are presented in Table 1.

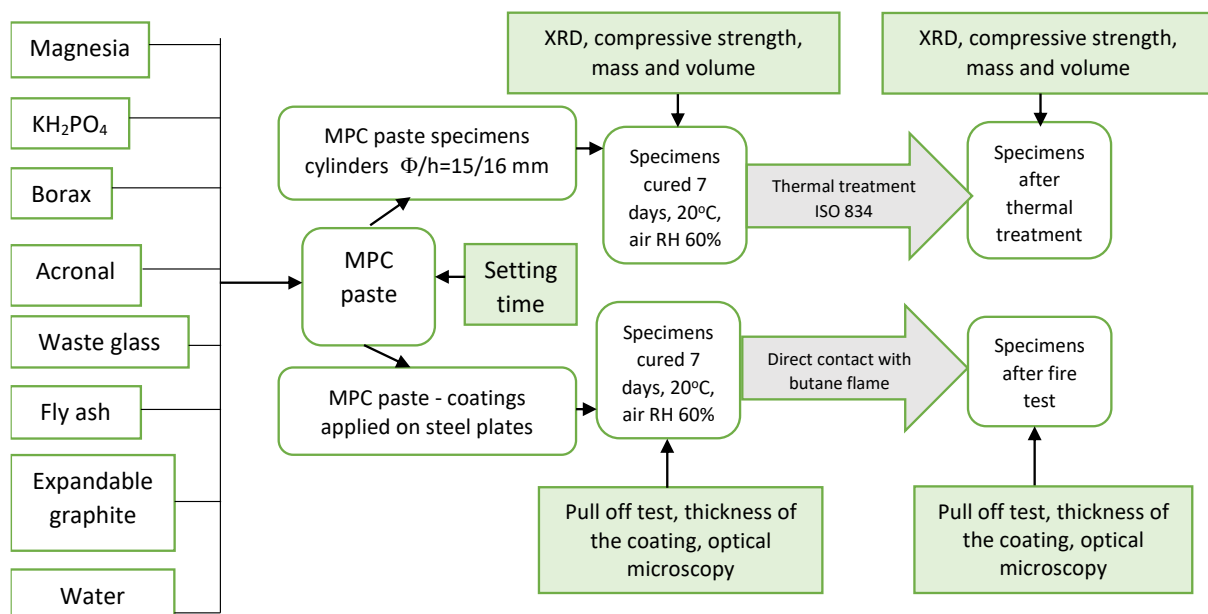
Table 1. The composition of studied phosphate cements (wt%).

Specimens	Magnesia (M)	KH ₂ PO ₄ (MKP)	Borax (B)	Acronal (Ac)	Waste Glass Powder (S)	Fly ash (F)	Expandable Graphite (EG) *
M	61	30	9	0	0	0	-
M_Ac	57	29	9	6	0	0	-
MS_Ac	54	27	7	6	6	0	-
MS_Ac_EG	54	27	7	6	6	0	0.67 *
MS_F_Ac	34	17	8	7	7	27	-

*) EG was calculated with reference to M content and was added to the mixture of other components.

The waste glass powder represents 10% and fly ash represents 40% of M + F + S. The water-to-solid ratio was 0.26 for M and M_Ac compositions, 0.25 for MS_Ac and MS_Ac_EG compositions, and 0.38 for the composition with waste glass and fly ash (MS_F_Ac).

The experimental program is presented in Figure 2.

**Figure 2.** Experimental program.

The setting time of MPC was assessed with Vicat apparatus equipped with Vicat needle [31]. The setting time represents the time elapsed from the moment when the MPC components were mixed and the moment when the Vicat needle leaves only a small imprint on the surface of the paste.

The compressive strengths were assessed on paste specimens (cylinders with 15 mm × 16 mm—diameter × height); the pastes were cured the first day in the mold, and after demolding were kept in air at 20 ± 2 °C for 7 days. The compressive strength was determined using a testing machine (Matest, Treviolo, Italy).

The adhesion strength was determined on coated plates, i.e., phosphate cement paste was applied on one face of the carbon steel plate (100 × 100 × 3 mm—length × width × height), which was previously mechanically treated (grinded) with sandpaper. On the hardened cement coating (average thickness of 2 mm), a square metallic pull-off head (l = 35 mm) was glued with epoxy binder and cured for 1 day in air. The adhesion strength of the cement coating to the steel substrate was assessed by dividing the maximum load recorded with a universal testing machine LFV 300 (Walter + Bai AG Löhningen, Switzerland) using a displacement-controlled test at 1 mm/min (Figure 3) to the cross-sectional area of the specimen.

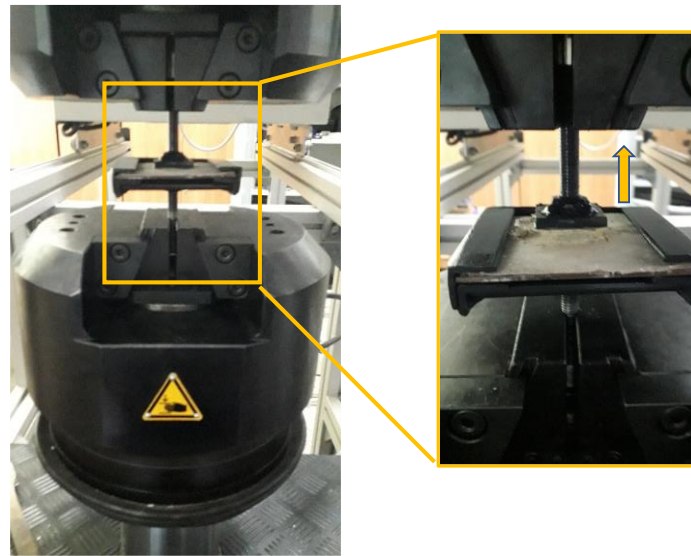


Figure 3. Pull-off test setup.

The X-ray diffraction (XRD) analyses were performed with an XRD 6000 Shimadzu diffractometer (Shimadzu, Kyoto, Japan), using $\text{CuK}\alpha$ ($\lambda = 1.5406 \text{ \AA}$) radiation with a scanning speed of $2^\circ/\text{min}$.

The SEM analyses were performed on a Quanta Inspect F scanning electronic microscope (1.2 nm resolution—Thermo Fisher, Eindhoven, The Netherlands).

The behavior of the studied MPCs at high temperatures was assessed in two ways:

- Thermal treatment (tt) of the paste specimens (cylinders with $15 \text{ mm} \times 16 \text{ mm}$ —diameter \times height), previously hardened for 7 days in air at 20°C , in an electric oven following the time–temperature curve presented in the international standard ISO 834 [32,33]; this thermal treatment is considered the most appropriate for the testing of construction materials subjected to a fire hazard based on the burning rate of general combustible building materials [32]. The maximum temperature was 1050°C and was achieved after 120 min. The mass, volume, and compressive strength of specimens were assessed before and after the thermal treatment.
- Direct contact with a butane flame applied of the MPC coatings applied on one side of a steel plate and recording the temperature on the opposite face (steel substrate). The distance between the torch head and the steel plate was kept constant (55 mm) in all the experiments. A detailed description of the test setup can be found in a previous paper [6]. The temperature of the steel substrate was measured for 1 h every 60 s using a pyrometer, with an accuracy of $\pm 1\%$ from the recorded value $+1^\circ\text{C}$.

The microstructure of the coatings (surface and area where the material was pulled off), before and after the contact with the flame, was assessed using an optical microscope DPM 300 digital pocket microscope (BYK-Gardner, Germany).

The modifications in volume, mass, or coating thickness after the thermal treatment or direct contact with the flame were calculated with the formula:

$$\Delta X = (X_a - X_b)/X_b - 100 (\%) \quad (1)$$

where

X_b = volume/mass/coating thickness before thermal treatment or direct contact with the flame;

X_a = volume/mass/coating thickness after thermal treatment or direct contact with the flame.

3. Results and Discussion

The setting times of the studied magnesium phosphate cements (MPCs) are presented in Figure 4. As can be seen, the setting of M paste is rapid (9 min and 30 s). The presence of the polymer suspension (Ac) in the composition M_Ac, slightly delays the setting of this composition (12 min and 30 s). This delay could be due to the partial adsorption of the polymer suspension (Ac) on the magnesia particles, thus slightly delaying their interaction with phosphate.

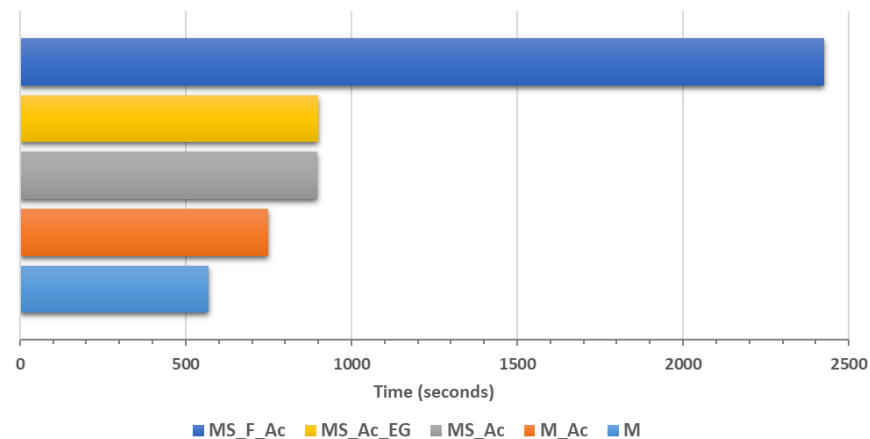


Figure 4. Setting times of the studied magnesium phosphate cement pastes.

The partial replacement of magnesia with waste glass powder (MS_Ac) delays the setting time, up to 14 min and 58 s, mainly due to the reduction of magnesia content; it is well known that MPC hardening is due to the reaction of magnesia with a potassium phosphate solution and $\text{KMgPO}_4 \cdot 6\text{H}_2\text{O}$ formation [13,18,20]. Furthermore, the increase in the substitution degree of magnesia with fly ash and waste glass powder up to 50% (MS_F_Ac) further delays the setting time of these cements due to the dilution effect as well as the increase in the water-to-solid ratio [34,35].

The thermal treatment (according to temperature–time curve stipulated in ISO 834:2019 standard) of MPC specimens, previously cured in air for 7 days, determines their contraction (see Figures 5 and 6). The replacement of magnesia with fly ash (F) or/and waste glass powder (S) reduces this contraction (Figure 6).

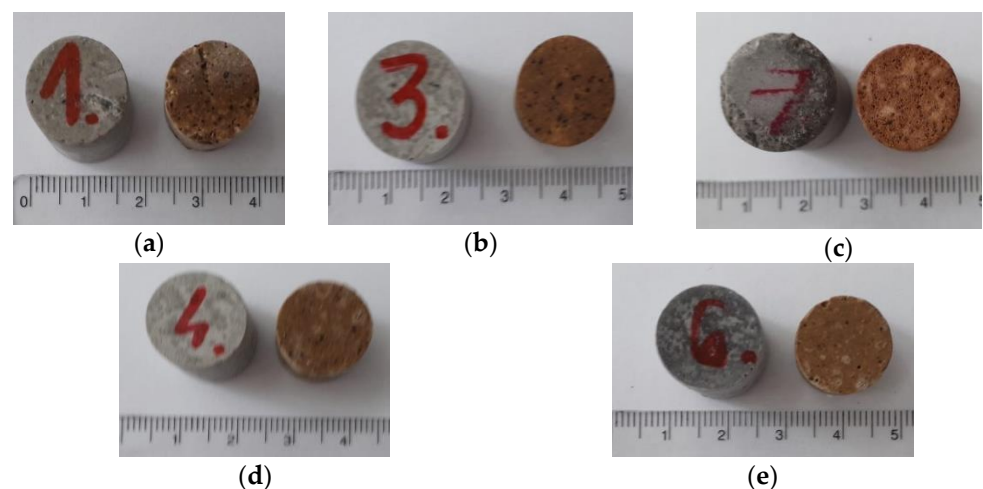


Figure 5. Visual aspect of the magnesium phosphate cement specimens before and after thermal treatment: (a) M, (b) M_Ac, (c) MS_F_Ac, (d) MS_Ac, and (e) MS_Ac_EG.

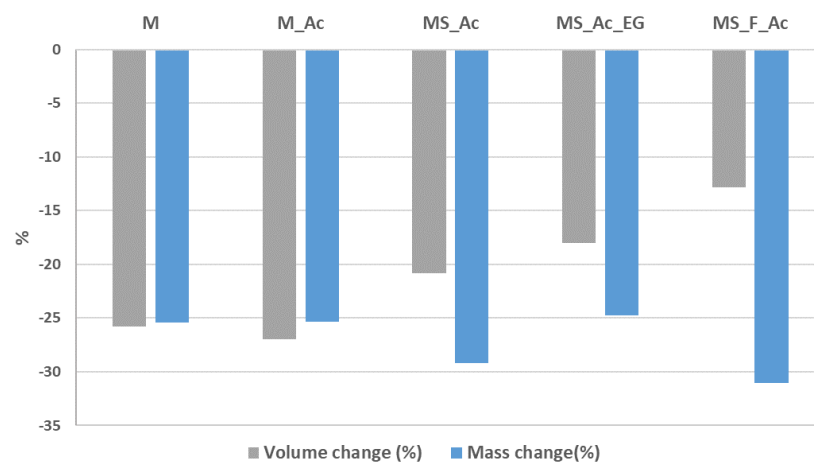


Figure 6. Volume and mass changes after the thermal treatment.

The important mass loss recorded for the cement paste with S and F content, as compared with M paste, can be explained by the processes which take place in these system when the thermal treatment (tt) is applied. According to the XRD patterns presented in Figure 7a,b, in the magnesium phosphate cements M and M_Ac, hardened for 7 days (before tt), the main crystalline hydrate formed is K-struvite ($\text{KMgPO}_4 \cdot 6\text{H}_2\text{O}$), which coexists with MgO (only part of magnesia reacted with the KH_2PO_4 solution to form K-struvite). The thermal treatment determined the dehydration of K-struvite and its transformation into KMgPO_4 [16,36].

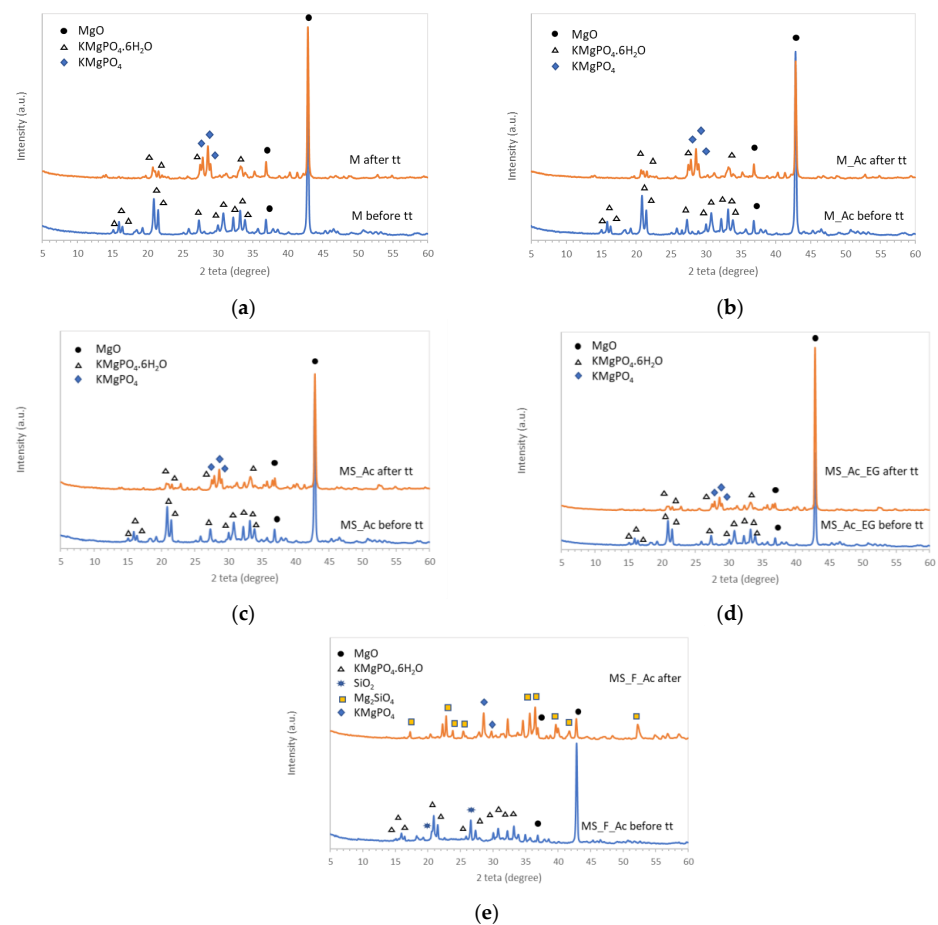


Figure 7. XRD patterns of the studied composition before and after the thermal treatment (tt): (a) M, (b) M_Ac, (c) MS_Ac, (d) MS_Ac_EG, and (e) MS_F_Ac.

The addition of waste glass powder, polymer suspension (Ac), or expandable graphite (EG) did not modify the nature of crystalline compounds assessed by XRD before and after the thermal treatment (Figure 7c,d).

On the XRD patterns of the composition in which magnesia is partially substituted (50 wt%) with waste glass powder and fly ash (MS_F_Ac—Figure 7e), one can assess in the cement paste, hardened for 7 days (before the thermal treatment), the presence of MgO, K-struvite, and SiO₂ (from fly ash). The thermal treatment at 1050 °C determined the of formation forsterite (Mg₂SiO₄) in the reaction of MgO with SiO₂. At the same time, KMgPO₄ resulting from K-struvite dehydration can be assessed on the XRD patterns of this composition (after tt).

The identification of forsterite by XRD analysis, only in one sample (MS_F_Ac), could be explained by the higher amount of silica available (both from glass and fly ash); therefore, the amount of forsterite formed is higher (as compared with the other MPCs with only 10% waste glass) and can be identified by this method. At the same time, one cannot exclude the possibility of forsterite formation in the MPCs with S addition, but its amount is probably much smaller (under the detection limit of the diffractometer).

The compressive strengths of the magnesium phosphate cements hardened for 7 days and after thermal treatment are presented in Figure 8. As can be seen, the addition of the polymer suspension (Ac) does not substantially modify the compressive strength values before the thermal treatment (tt), which is opposite to the substitution of magnesia with waste glass powder (S) and fly ash (F). In this case, the compressive strength decreases by 9% for the composition with 10% S (MS_Ac), and is very small when 50% of magnesia is substituted with S and F. This was to be expected given the fact that the reduction of magnesia content determines the reduction of K-struvite formed by the reaction of MgO and KH₂PO₄ solution. K-struvite, the main crystalline hydrate formed in this type of cement, is also the main component that determines the hardening and increase in the compressive strength values.

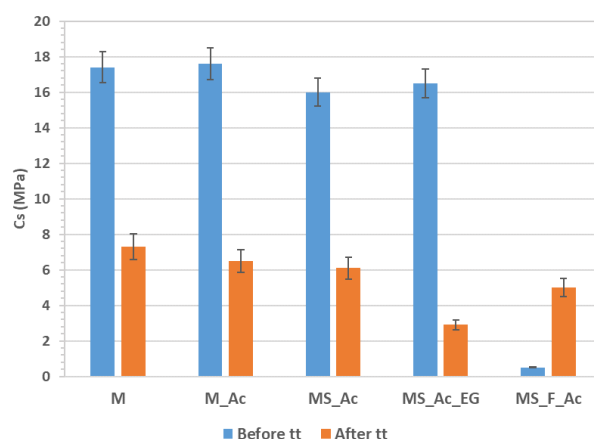


Figure 8. Compressive strength before and after thermal treatment (tt) performed according to the ISO 834 curve.

Moreover, due to the presence of porous particles in the fly ash (see Figure 9a–c) and the high content of fine particles (Figure 9d), the water dosage for the pastes with F content increased up to a water-to-solid ratio = 0.38, in order to keep an adequate workability of the fresh paste. The increase in water dosage is detrimental for the compressive strength of hardened paste due to the porosity increase.

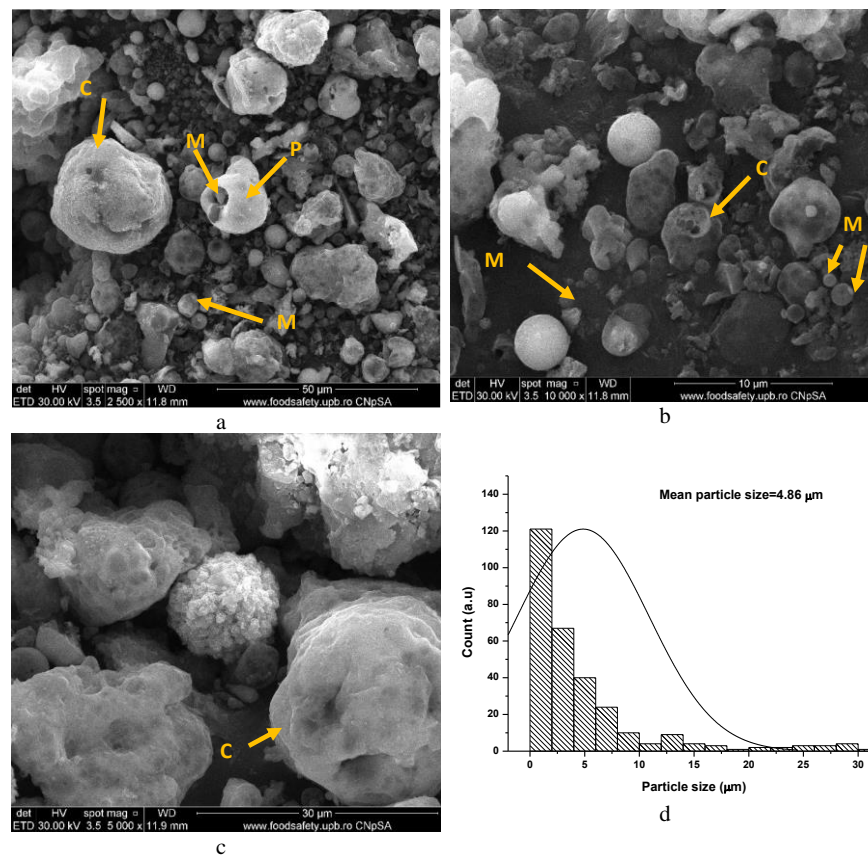


Figure 9. SEM images (a–c) and particle-size distribution of fly ash (d).
















One can notice in Figure 9, a plerosphere (P), i.e., a hollow round particle which is filled with microspheres (M), and cenospheres (C), i.e., hollow particles (with continuous or porous surface) with different sizes [37].

The thermal treatment (tt) has a different influence on the volume and mass of the MPC pastes (Figure 6) in correlation with the physical and chemical changes which occur in these compositions when the temperature increases. When the main hydrate present in the system is K-struvite (M, M_Ac, MS_Ac, MS_Ac_EG), the tt determines its dehydration—a process that leads to a significantly lower volume of the solid phase and, thus, to a lower compressive strength of the material [38], as can be seen in Figure 8.

For the composition with fly ash (MS_F_Ac), the compressive strength increases after thermal treatment, most probably due to the formation of a higher amount of forsterite, a compound with good mechanical properties (fracture toughness and hardness) [39].

The direct contact of the MPC coatings applied on steel plates with the flame determines changes in the coating's visual aspect (Table 2) as well as the increase in the substrate (steel plate) temperature (Figure 10).

Table 2. The visual aspects of the steel plate covered with studied MPCs, before, during, and after direct contact with the butane flame for 60 min.

Specimen	Before	During	After
M			
M_Ac			
MS_Ac			
MS_Ac_EG			
MS_F_Ac			

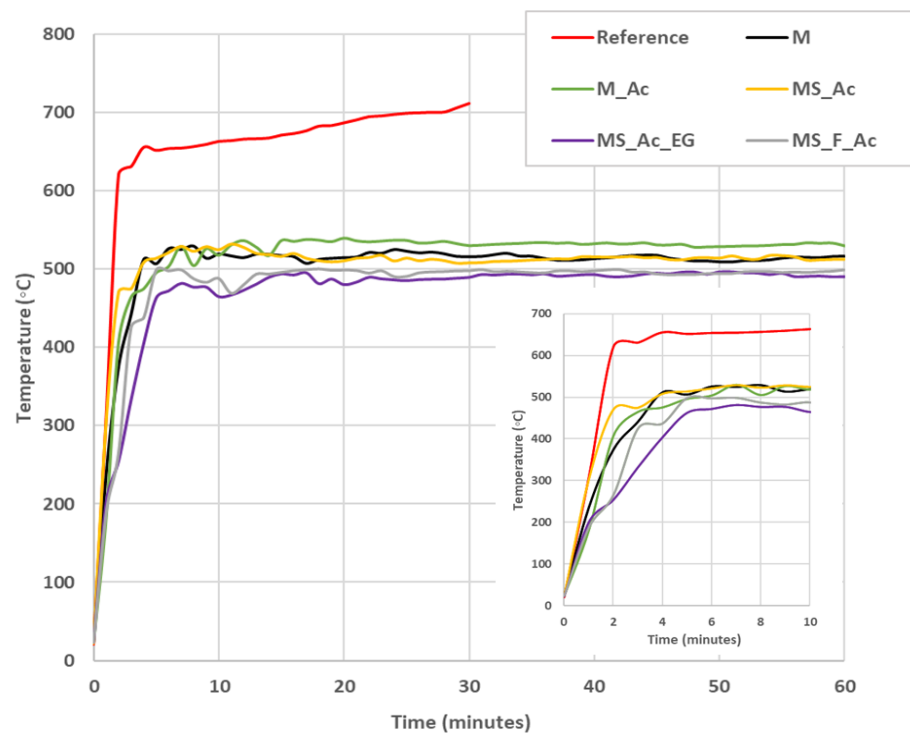


Figure 10. Substrate (steel plate) temperature vs. contact time with the flame. Reference—uncoated steel plate.

As can be seen from Table 2, the studied MPC coatings do not present delamination after direct contact with the flame. The visual aspect of coating M did not change during the contact with the flame (in the contact area), but cracks can be visually assessed in this coating, mainly in the adjacent areas of the one which was in direct contact with the flame.










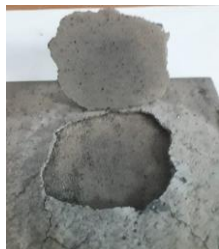
For the compositions with an Ac addition, one can notice the darkening of the coating during contact with the flame, most probably due to the burning of this polymer. The addition of waste glass (MS_Ac and MS_Ac_EG) leads to partial melting of the coating (sinterization) in the area where it was in direct contact with the flame; this was to be expected given the melting point of soda–lime glass (generally below 1000 °C) [40]. For the composition with fly ash content (MS_F_Ac), one can also notice a small local swelling of the coating in the area where the flame was in direct contact with the material.

The temperature of the substrate (steel plate) assessed on the opposite side of the one coated with MPCs vs. the contact time with the flame is presented in Figure 10. As can be seen, for the uncoated steel plate (reference), the temperature of the substrate abruptly increases to 600 °C in the first 2 min and then increases with a lower rate up to 700 °C. The substrate temperature of the plates coated with MPCs also presents a sharp increase in the first 2–6 min (see insert in Figure 10), but after that, it stabilizes around 500 °C. The lowest maximum temperature, around 490 °C, was assessed for the steel plate coated with MS_Ac_EG.

When the fly ash is also present in the MPC formulation (MS_F_Ac), the rate of the temperature increase in the steel substrate is lower as compared to the previously discussed samples, but the maximum temperature achieved is still high (around 500 °C).

The visual aspects and the type of fracture assessed by a pull-off test of the MPC coatings (before and after the direct contact with the flame) are presented in Table 3.

Table 3. Visual aspects of the steel plate covered with the studied MPCs, after pull-off test. This test was performed on the MPC coatings before and after the fire test.

Specimen	Before Fire Test		After Fire Test	
	Visual Aspect	Type of Fracture	Visual Aspect	Type of Fracture
M		Partial adhesive/cohesive		Cohesive
M_Ac		Adhesive		Partial adhesive/cohesive
MS_Ac		Partial adhesive/cohesive		Cohesive
MS_Ac_EG		Adhesive		Cohesive
MS_F_Ac		Adhesive		Adhesive *

* The coating swelled in the contact area with the flame, and a local delamination from the steel substrate occurred. On the surface of the steel plate, a thin layer of coating is still present.

As can be seen, the M cement has a good adhesion to the steel substrate before contact with the flame. According to data from the literature, this good adhesion could be due to a phosphating film which is formed at the steel–MPC interface and can contain $\text{FeH}(\text{H}_2\text{PO}_4)_2$

and FePO_4 as main products [17,18]. This film, located at the interface between the steel plate and coating layer, also exerts a protective effect on steel corrosion [17].

After contact with the flame, the M coating's failure becomes cohesive, which could be due to an increase in the adhesion strength (Figure 11a).

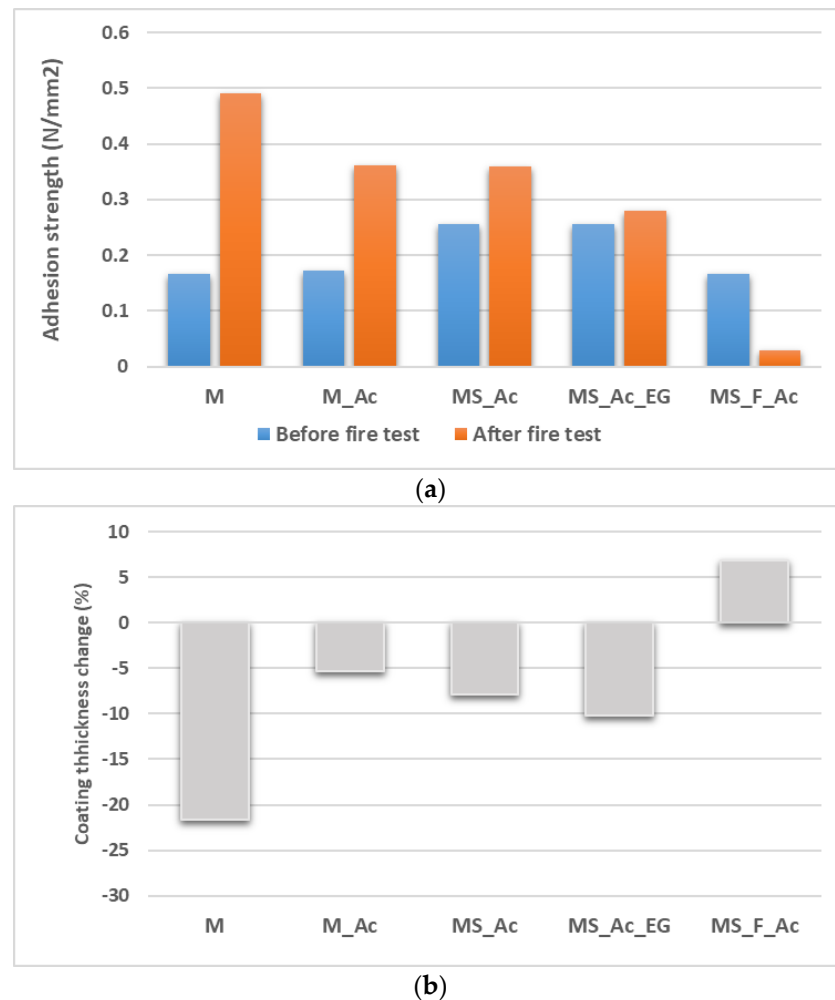


Figure 11. (a) Adhesion strength of phosphate cement coatings to the steel plate, before and after direct contact with the flame for 1 h, and (b) changes in the thickness of the coatings (in the area which was in direct contact with the flame).

The addition of the polymer suspension (Ac) did not improve the adhesion to the steel substrate; an adhesive failure of the M_Ac coating (at the interface of the coating–steel substrate) occurred before the fire test. After the fire test, the failure becomes partially cohesive, and the adhesion strength increases (see Figure 11a). Several factors could determine this behavior, i.e., the decrease in the mechanical strength of this material (Figure 6) correlated with a lower contraction of this coating compared with the M coating (Figure 11b).

The partial replacement of magnesia with waste glass powder (MS_Ac) improves the adhesion strength to the metal substrate before the fire test. The decrease in this material's compressive strength after the thermal treatment (Figure 6) could be an explanation for the cohesive fracture of this coating.

For the MPC coating with waste glass and fly ash content (MS_F_Ac), the failure mode is adhesive before the fire test. After the contact with the flame, due to local swelling of the coating in the contact zone with the flame (see also Figure 11b) and probably local delamination, the adhesion strength dramatically decreases (Figure 11a).

The microstructures of the coating surface and of the region where the coating was pulled off from the steel plate, before and after contact with the flame, are presented in Figures 12–16.

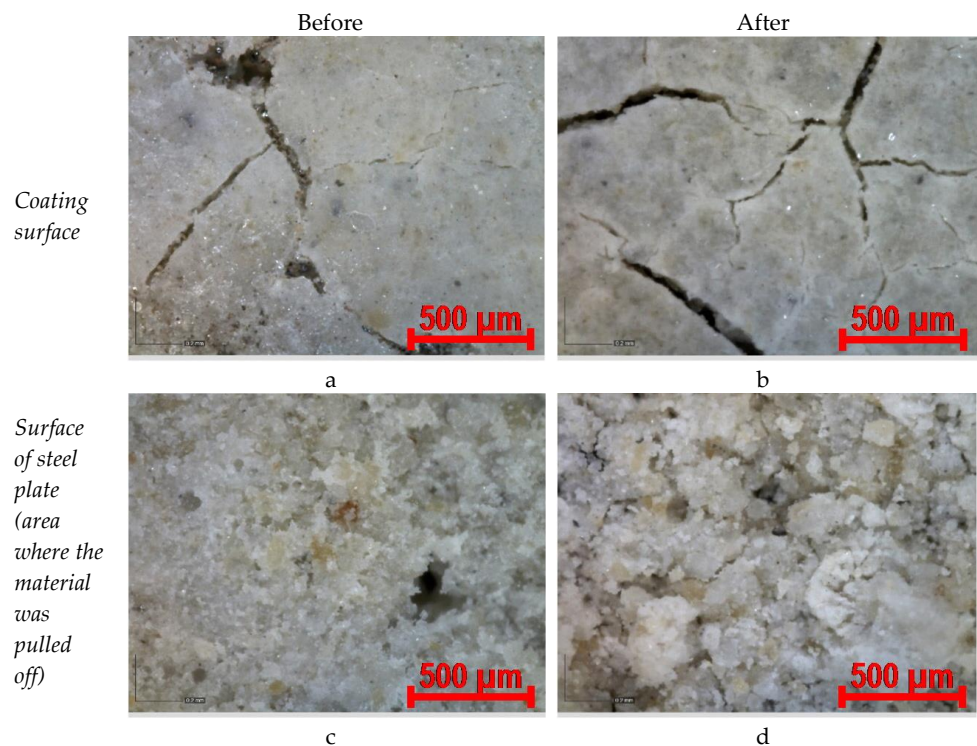


Figure 12. Optical microscopy images of coating M, before and after contact with the flame (magnification $\times 220$): (a,c) before fire test; (b,d) after fire test.

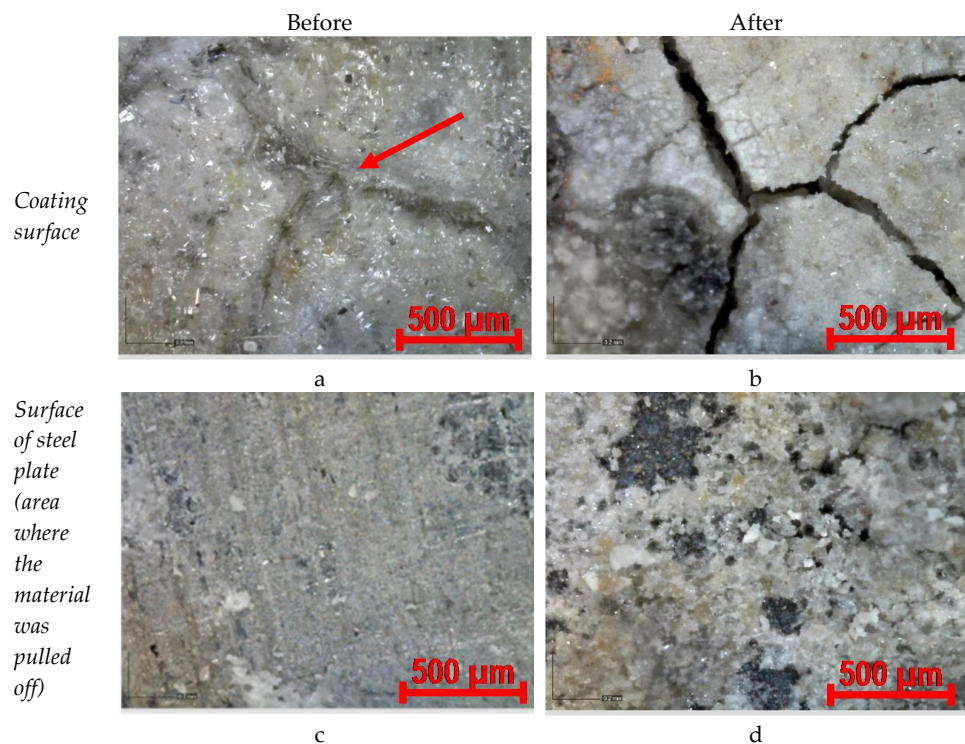


Figure 13. Optical microscopy images of coating M_Ac, before and after contact with the flame (magnification $\times 220$): (a,c) before fire test; (b,d) after fire test.

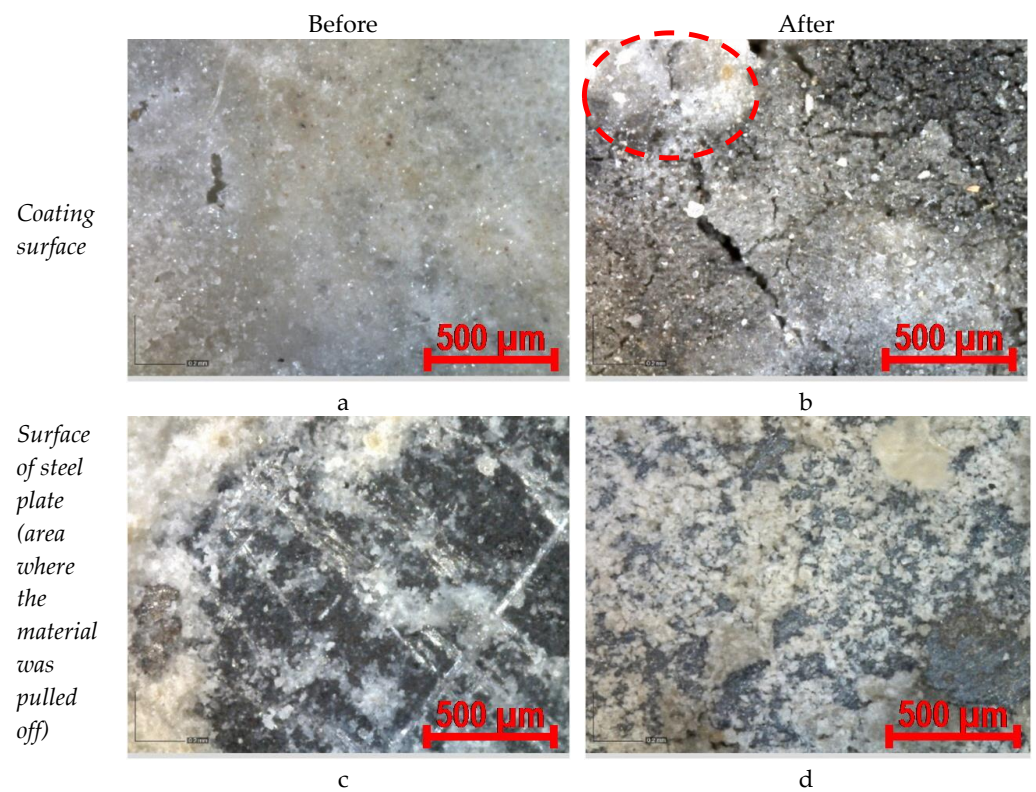


Figure 14. Optical microscopy images of coating MS_Ac, before and after contact with the flame (magnification $\times 220$): (a,c) before fire test; (b,d) after fire test.

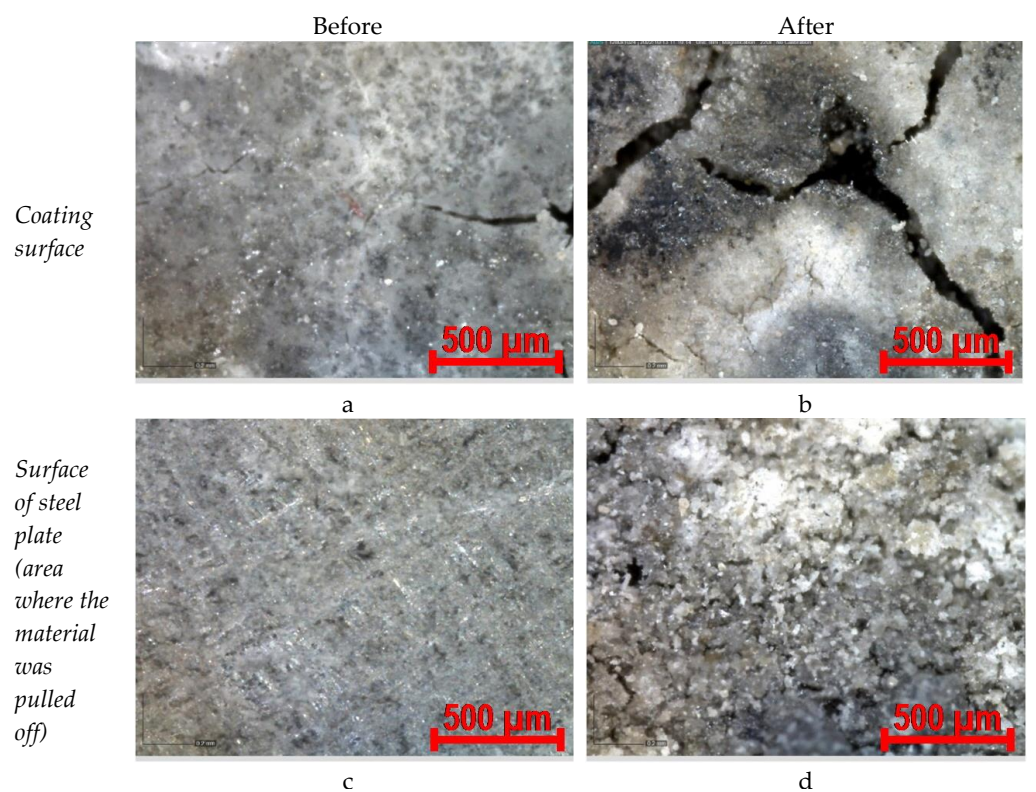


Figure 15. Optical microscopy images of coating MS_Ac_EG, before and after contact with the flame (magnification $\times 220$): (a,c) before fire test; (b,d) after fire test.

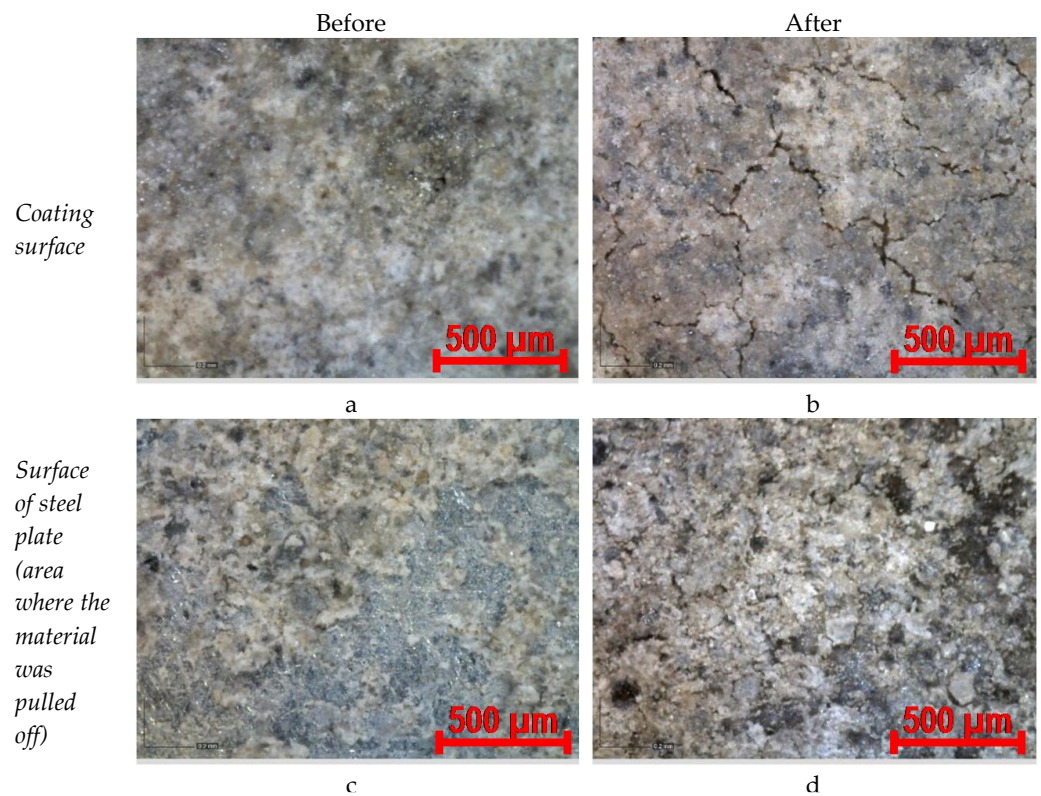


Figure 16. Optical microscopy images of coating MS_F_Ac, before and after contact with the flame (magnification $\times 220$): (a,c) before fire test; (b,d) after fire test.

As can be seen from Figure 12a, microcracks can be assessed on the surface of the M coating even before contact with the flame. These microcracks can be due to the superficial drying of the M coating. On the surface of the steel plate (in the area where the material was pulled off), a thick layer of material is still present. After contact with the flame, the number and sizes of cracks present on the coating surface increase (some of them can also be visually assessed), but the material remains well-adhered to the surface of the steel plate (Figure 12d), and the fracture occurs in the material, not at the steel plate–coating interface (see also Table 3).

The addition of a styrene–acrylic dispersion (Ac) seems to improve the elasticity of the coating and mitigate its cracking (see one microcrack partially filled/bound by the polymer—arrow in Figure 13a). Still, the adhesion of this coating to the steel substrate is much lower, the failure becomes adhesive, and the surface of the steel plate is virtually not covered anymore with material (Figure 13c). The contact with the flame determines the occurrence of more microcracks on the coating’s surface, most probably due to the burning of the polymer when the coating’s temperature (and substrate) increases; still, the coating’s adherence to the steel substrate is improved, and more material remains attached at the surface of steel plate (partial cohesive failure—see also Table 3).

The partial replacement of the magnesia with waste glass powder (MS_Ac—Figure 14) does not substantially modify the aspect of the coating but seems to improve the bonding to the steel substrate—more material remains attached at the surface of the steel plate after the pull-out test (Figure 14c). The contact with the flame also determines the occurrence of microcracks at the surface of the coating, but the partial melting of glass particles seems to stop the development of cracks (see the dotted circle in Figure 14b). The adherence to the steel plate increases, and more material remains adhered to the surface of the steel plate.

The addition of EG (Figure 15) does not seem to substantially change the microstructure of this coating; after contact with the flame, microcracks are visible on the surface of the coating, but one cannot assess any local expansion determined by the EG. This could be

due to the low amount of this addition as well as to the higher stiffness of the MPC coating compared to polymer-based coatings or alkali-activated glass materials, which soften and melt at lower temperatures [29].

The microstructure of the MPC with fly ash content is presented in Figure 16. The important decrease in the adhesive bond strength (Figure 11a) can be explained by the decrease in the K-struvite amount formed in these systems. Nevertheless, at the surface of the steel plate (Figure 16c), one can also assess in some regions a very thin layer of material that remained adhered after the pull-out test. After contact with the flame, numerous microcracks can be assessed on the coating's surface, but the layer of material still adhered to the surface of the steel plate is thicker and almost continuous. This is the consequence of the local swelling of the material during the contact with the flame (see also Figure 11b and Table 3), which most probably occurred in the material and not at the interfacial transition zone between the steel plate and coating.

4. Conclusions

The composition of magnesium phosphate cements (MPCs) can be modified to improve several properties which are important when used as passive fire protection materials.

The addition of styrene–acrylic dispersion (Acronal) or/and the glass powder extends the MPC's setting time. The magnesia substitution with waste glass powder and fly ash (50% wt.), combined with the addition of a polymer suspension (Ac) and an increase in the water-to-solid ratio, determines an important delay of the MPC setting time.

The thermal treatment of MPC specimens up to 1050 °C (applied according to temperature–time curve stipulated in the ISO 834:2019 standard) determines their contraction as well as an important mass loss (25–33%). These changes can be correlated with the modification in the mineralogical composition of the studied MPCs; for the MPCs with waste glass powder and without/with the addition of Ac, the main changes assessed by the X-ray diffraction analysis consist of the dehydration of K-struvite—the main reaction product resulting from the reaction of MgO with KH_2PO_4 solution. When the magnesia substitution rate is 50% wt., due to the presence of both waste glass powder and fly ash in the system, the thermal treatment at 1050 °C also leads to the formation of forsterite (Mg_2SiO_4) in the reaction of MgO (not entirely consumed in the reaction with KH_2PO_4 solution) with SiO_2 .

The compressive strengths of magnesium phosphate cements, before and after thermal treatment, are correlated with their mineralogical composition. The reduction of magnesia content in the MPCs (due to partial substitution with fly ash and/or waste glass powder) determines an important reduction in the initial compressive strength (before thermal treatment) correlated with the lower K-struvite content. When the main hydrate present in the hardened paste is K-struvite, the thermal treatment determines its dehydration, a process that decreases the compressive strength of the material. For the compositions with waste glass powder and fly ash, an increase in the compressive strength was recorded after thermal treatment, most probably due to the formation of a higher amount of forsterite, a compound with good mechanical properties.

The direct contact with a butane flame of the studied MPC coatings applied on steel plates determines the sharp increase in the steel plate (substrate) temperature in the first 4–6 min, but afterward, the temperature is stabilized around 490–500 °C; these temperatures are 30% lower compared to the temperature assessed for non-coated steel plates.

The adhesion strengths of the studied MPC coatings to the steel substrate were good, and no delamination was visually noticed during and after the contact with the flame. For the composition with fly ash content, the local swelling of the coating in the contact area with the flame determined a drastic decrease in the adhesion strength. The addition of a styrene–acrylic dispersion (Ac) improved the initial elasticity of the MPC coatings (before the fire test), and fewer microcracks were visible on the surface of these coatings compared to the one with plain MPC (without Ac addition).

Author Contributions: Conceptualization, N.F.C. and A.B.; Investigation, N.F.C., A.C.B. and R.C.C.; Methodology, N.F.C., A.B. and G.V.; Supervision, A.B. and G.V.; Writing—original draft N.F.C. and

A.B.; Writing—review and editing, A.B., G.V., A.C.B. and R.C.C. All authors have read and agreed to the published version of the manuscript.

Funding: This research received no external funding.

Institutional Review Board Statement: Not applicable.

Informed Consent Statement: Not applicable.

Data Availability Statement: Not applicable.

Conflicts of Interest: The authors declare no conflict of interest.

References

1. Lucherini, A.; Maluk, C. Intumescent coatings used for the fire-safe design of steel structures: A review. *J. Constr. Steel Res.* **2019**, *162*, 105712. [\[CrossRef\]](#)
2. EN 1993-1-2:2005; Eurocode 3 Design of Steel Structures—Part 1, 2: General Rules—Structural Fire Design. Comité Européen de Normalization (CEN): Brussel, Belgium, 2005.
3. Puri, R.; Khanna, A. Intumescent coatings: A review on recent progress. *J. Coat. Technol. Res.* **2017**, *14*, 1–20. [\[CrossRef\]](#)
4. Laím, L.; Caetano, H.; Santiago, A. Review: Effects of nanoparticles in cementitious construction materials at ambient and high temperatures. *J. Build. Eng.* **2021**, *35*, 102008. [\[CrossRef\]](#)
5. Nicoara, A.; Badanoiu, A.; Voicu, G.; Dinu, C.; Ionescu, A. Intumescent coatings based on alkali-activated borosilicate inorganic polymers. *J. Coat. Technol. Res.* **2020**, *17*, 681–692. [\[CrossRef\]](#)
6. Cirstea, N.; Badanoiu, A.; Boscornea, A. Intumescent Silicate Coatings with the Addition of Alkali-Activated Materials. *Polymers* **2022**, *14*, 1937. [\[CrossRef\]](#)
7. Kazmina, O.; Lebedeva, E.; Mitina, N.; Kuzmenko, A. Fire-proof silicate coatings with magnesium-containing fire retardant. *J. Coat. Technol. Res.* **2018**, *15*, 543–554. [\[CrossRef\]](#)
8. Nicoara, A.; Badanoiu, A.; Balanoiu, M.; Mathias, A.; Voicu, G. Alkali activated mortars with intumescent properties. *Rev. De Chim.* **2019**, *70*, 431–437. [\[CrossRef\]](#)
9. Nicoara, A.; Badanoiu, A. Influence of Alkali Activator Type on the Hydrolytic Stability and Intumescence of Inorganic Polymers Based on Waste Glass. *Materials* **2011**, *15*, 2011. [\[CrossRef\]](#)
10. Saadi, T.A.; Badanoiu, A.; Nicoara, A.; Stoleriu, S.; Voicu, G. Synthesis and properties of alkali activated borosilicate inorganic polymers based on waste glass. *Constr. Build. Mater.* **2017**, *136*, 298–306. [\[CrossRef\]](#)
11. Jia, G.; Li, Z. Influence of the aerogel/expanded perlite composite as thermal insulation aggregate on the cement-based materials. *Constr. Build. Mater.* **2021**, *273*, 121728. [\[CrossRef\]](#)
12. Karatas, M.; Benli, A.; Toprak, H. Effect of incorporation of raw vermiculite as partial sand replacement on the properties of self-compacting mortars. *Constr. Build. Mater.* **2019**, *221*, 163–176. [\[CrossRef\]](#)
13. Vijan, C.A.; Badanoiu, A.; Voicu, G.; Nicoara, A. Phosphate Cements Based on Calcined Dolomite: Influence of Calcination Temperature and Silica Addition. *Materials* **2021**, *14*, 3838. [\[CrossRef\]](#) [\[PubMed\]](#)
14. Dai, X.; Qian, J.; Qin, J.; Yue, Y.; Zhao, Y.; Jia, X. Preparation and Properties of Magnesium Phosphate Cement-Based Fire Retardant Coating for Steel. *Materials* **2022**, *15*, 4134. [\[CrossRef\]](#) [\[PubMed\]](#)
15. Fang, Y.; Cui, P.; Ding, Z.; Zhu, J. Properties of a magnesium phosphate cement-based fire-retardant coating containing glass fiber or glass fiber powder. *Constr. Build. Mater.* **2018**, *162*, 553–556. [\[CrossRef\]](#)
16. Vijan, A.; Badanoiu, A.; Voicu, G.; Nicoara, A. Coatings Based on Phosphate Cements for Fire Protection of Steel Structures. *Materials* **2021**, *14*, 6213. [\[CrossRef\]](#)
17. Wang, X.; Hu, X.; Yang, J.; Chong, L.; Shi, C. Research progress on interfacial bonding between magnesium phosphate cement and steel: A review. *Constr. Build. Mater.* **2022**, *342*, 127925. [\[CrossRef\]](#)
18. Wagh, A. Chemically Bonded Phosphate Ceramics: Twenty-First Century Materials with Diverse Applications. In *Chemically Bonded Phosphate Ceramics*; Elsevier: Amsterdam, The Netherlands, 2016.
19. Yang, Q.; Zhu, B.; Zhang, S.; Wu, X. Properties and applications of magnesia—Phosphate cement mortar for rapid repair of concrete. *Cem. Concr. Res.* **2000**, *30*, 1807. [\[CrossRef\]](#)
20. Vijan, C.; Badanoiu, A. The influence of potassium phosphate and fly ash addition on the setting time and mechanical strengths of magnesium phosphate cements. *UPB Sci. Bull.* **2020**, *82*, 21–32.
21. Yang, Q.; Zhu, B.; Wu, X. Characteristics and durability test of magnesium phosphate cement-based material for rapid repair of concrete. *Mater. Struct.* **2000**, *33*, 229–234. [\[CrossRef\]](#)
22. Qiao, F.; Chau, C.; Li, Z. Property evaluation of magnesium phosphate cement mortar as patch repair material. *Constr. Build. Mater.* **2010**, *24*, 695–700. [\[CrossRef\]](#)
23. Brückner, T.; Meininger, M.; Groll, J.; Kübler, A.; Gbureck, U. Magnesium Phosphate Cement as Mineral Bone Adhesive. *Materials* **2019**, *12*, 3819. [\[CrossRef\]](#) [\[PubMed\]](#)
24. Ostrowski, N.; Roy, A.; Kumta, P. Magnesium Phosphate Cement Systems for Hard Tissue Applications: A Review. *ACS Biomater. Sci. Eng.* **2016**, *2*, 1067–1083. [\[CrossRef\]](#) [\[PubMed\]](#)

25. Mestres, G.; Aguilera, F.; Manzanares, N.; Sauro, S.; Osorio, R.; Toledano, M.; Ginebra, M. Magnesium phosphate cements for endodontic applications with improved long-term sealing ability. *Int. Endod. J.* **2014**, *47*, 127–139. [[CrossRef](#)]
26. Zárýbnická, L.; Machotová, J.; Mácová, P.; Machová, D.; Viani, A. Design of polymeric binders to improve the properties of magnesium phosphate cement. *Constr. Build. Mater.* **2021**, *290*, 123202. [[CrossRef](#)]
27. Li, Y.; Bai, W.; Shi, T. A study of the bonding performance of magnesium phosphate cement on mortar and concrete. *Constr. Build. Mater.* **2017**, *142*, 459–468. [[CrossRef](#)]
28. Deng, Q.; Lai, Z.; Xiao, R.; Wu, J.; Liu, M.; Lu, Z.; Lv, S. Effect of Waste Glass on the Properties and Microstructure of Magnesium Potassium Phosphate Cement. *Materials* **2021**, *14*, 2073. [[CrossRef](#)]
29. Saadi, T.A.; Mohammad, S.; Daway, E.; Mejbil, M.K. Synthesis of intumescent materials by alkali activation of glass waste using intercalated graphite additions. *Mater. Today Proc.* **2021**, *42*, 1889–1900. [[CrossRef](#)]
30. Hung, W.; Wu, K.; Lyu, D.; Cheng, K.; Huang, W. Preparation and characterization of expanded graphite/metal oxides for antimicrobial application. *Mater. Sci. Eng. C* **2017**, *75*, 1019–1025. [[CrossRef](#)]
31. EN 196-3:2016; Methods of Testing Cement—Part 3: Determination of Setting Times and Soundness. CEN: Brussels, Belgium, 2016. Available online: <https://standards.iteh.ai/catalog/standards/cen/e4921eca-8101-4261-b066-25d19b9b8e8a/en-196-3-2016> (accessed on 20 October 2022).
32. Panchego-Torgal, F.; Labrincha, J.L.C.; Palomo, A.; Chindaprasirt, P. *Handbook of Alkali-Activated Cements, Mortars and Concretes*; Elsevier Ltd.: Cambridge, UK, 2015.
33. Baux, C.; Mélinge, Y.; Lanos, C.; Jaubertie, R. Enhanced Gypsum Panels for Fire Protection. *J. Mater. Civ. Eng.* **2008**, *20*, 71–77. [[CrossRef](#)]
34. Li, Y.; Chen, B. Factors that affect the properties of magnesium phosphate cement. *Constr. Build. Mater.* **2013**, *47*, 977–983. [[CrossRef](#)]
35. Yang, Y.; Fang, B.; Zhang, G.; Guo, J.; Liu, R. Hydration Performance of Magnesium Potassium Phosphate Cement Using Sodium Alginate as a Candidate Retarder. *Materials* **2022**, *15*, 943. [[CrossRef](#)] [[PubMed](#)]
36. Gardner, L.J.; Walling, S.A.; Lawson, M.S.; Sun, S.; Bernal, S.A.; Corkhill, C.; Provis, J.L.; Apperley, D.; Dinu Iuga, D.; Hanna, J.; et al. Characterization of and Structural Insight into Struvite-K, MgKPO₄·6H₂O, an Analogue of Struvite. *Inorg. Chem.* **2021**, *60*, 195–205.
37. Goodarzi, F.; Sanei, H. Plerosphere and its role in reduction of emitted fine fly ash particles from pulverized coal-fired power plants. *Fuel* **2009**, *88*, 382–386. [[CrossRef](#)]
38. Xu, B.; Winnefeld, F.; Lotenbach, B. Effect of temperature curing on properties and hydration of wollastonite blended magnesium potassium phosphate cements. *Cem. Concr. Res.* **2021**, *142*, 106370. [[CrossRef](#)]
39. Saidy, R.; Fathi, M.; Salimijazi, H.; Mohammadrezaie, M. Fabrication and characterization nanostructured forsterite foams with high compressive strength, desired porosity and suitable bioactivity for biomedical applications. *J. Sol-Gel Sci. Technol.* **2017**, *81*, 734–740. [[CrossRef](#)]
40. Xie, Z.; Xi, Y. Use of recycled glass as a raw material in the manufacture of Portland cement. *Mater. Struct.* **2002**, *35*, 510–515.